

S. A. Solman · C. G. Menéndez

Weather regimes in the South American sector and neighbouring oceans during winter

Received: 27 September 2002 / Accepted: 27 January 2003 / Published online: 2 April 2003
© Springer-Verlag 2003

Abstract We classified 34 years of winter daily 500 hPa geopotential height patterns over the eastern South Pacific–South America–South Atlantic region using the K-means clustering method. We found a significant classification into five weather regimes (WRs) defined as the most frequent large-scale circulation anomalies: WR1 (trough centred downstream of the Drake Passage), WR2 (trough over the SW Pacific and ridge downstream), WR3 (ridge over the SE Pacific and NW–SE trough downstream), WR4 (trough over the SE Pacific and NW–SE ridge downstream) and WR5 (weak ridge to the west of southern South America). We also analysed their persistence and temporal evolution, including transitions between them and development around onsets and breaks of each regime. The preferred transitions, WR1 → WR3 → WR2 → WR4 → WR1 and also WR1 → WR3 → WR2 → WR1, suggest the progression of a Rossby wave-like pattern in which each of the regimes resemble the Pacific–South America modes. Significant influence of the WRs on local climate over Argentina was found. The preferred transitions WR1 → WR3 and WR3 → WR2 induce sustained cold conditions over Patagonia and over northern Argentina, respectively. The most significant change in precipitation frequency is found for WR3, with wetter conditions over all the analysed regions. Finally, the interannual to interdecadal significant variations in the occurrence of these regimes were discussed. WR1 and WR3 are more frequent and WR2 is less frequent during El Niño, and WR2 and WR5 are more frequent and WR1 is less frequent during La Niña. A significant decrease in WR2 and increase of WR4 and WR5 during the 1970s and early 1980s were found.

1 Introduction

Wintertime extratropical atmospheric flows are characterised by certain large-scale patterns that appear recurrently at fixed locations remaining beyond the lifetime of individual synoptic-scale systems. A large part of the intraseasonal variability of the Southern Hemisphere (SH) is related to the alternating between such large-scale circulation patterns. Previous studies found that the leading modes of both intraseasonal and interannual variability over the SH display a dominance of wave 3 and 4 structures, with fluctuations in similar locations on a broad range of time scales (Kiladis and Mo 1998). The low-frequency variability consists basically of a mid- to high-latitude vacillation in the zonal wind strength (the high-latitude mode, Kidson 1988) and two eastward propagating wave 3 modes in quadrature with each other. These represent Rossby wave trains over the South Pacific characterised by a wave-like pattern extending from the central Pacific arching to Argentina and propagating equatorward into the Atlantic Ocean. They are referred to as the Pacific–South American modes (Ghil and Mo 1991; Mo and Higgins 1998) and represent the main modes of low-frequency oscillation in the SH (nevertheless, it should be mentioned that these are not the only Rossby wave patterns that propagate in these regions).

Extratropical atmospheric flow regimes, or weather regimes (WRs), can be described in terms of geographically fixed large-scale circulation anomalies that appear intermittently or episodically. There are several approaches to classify WRs based on their different properties: persistence, recurrence, and quasi-stationarity (see review by Michelangeli et al. 1995; MVL hereafter). Though different techniques exist for classifying WRs, basically those devoted to find the states that maximise the probability density function (e.g. Kimoto and Ghil 1993; Robertson and Ghil 1999), those in which WRs are defined as quasi-stationary states of the atmospheric circulation (e.g. Vautard 1990) and those in which recurrent

S. A. Solman (✉) · C. G. Menéndez
Centro de Investigaciones del Mar y la Atmósfera (CIMA-
CONICET/UBA) – Dto. Cs. de la Atmósfera y los Océanos (UBA)
Ciudad Universitaria – Pabellón II 2° piso (1428) Buenos Aires –
Argentina
E-mail: solman@at.fcen.uba.ar

patterns are identified (e.g. MVL; Plaut and Simonnet 2001), in fact there is no optimal way of classifying WRs. Moreover, some of the papers mentioned found that WRs obtained using different techniques are quite similar. The literature in which these techniques have been largely applied focused mainly on the North Atlantic and North Pacific circulation patterns.

One major aim of this study is to identify the WRs over the eastern South Pacific-South America-South Atlantic region, their persistence, and their temporal evolution including transitions between WRs and development around onsets and breaks of each regime. We define WR as the most frequently occurring patterns and we apply the K-means clustering method based on pattern recurrence as used by MVL. This is a partitioning method that classifies all days into a predefined number of clusters and the method minimises the variance within the set of clusters. Descriptions of the rapid transitions between the WRs, associated with the nonlinearity of the atmospheric dynamics are necessary in order to complete the picture of the climate variability in the region.

Synoptic activity, which determines local weather, is influenced by the atmospheric large-scale patterns and in particular by their amplitude and location. Therefore, another motivation is to investigate the linkage between WRs and local weather patterns over Argentina. This approach provides a worthy starting point for a down-scaling method to local weather (e.g. Robertson and Ghil 1999; Plaut and Simonnet 2001), characterised by e.g. surface temperature and precipitation.

Finally, we also investigate the relationships between WRs and lower-frequency variability (interannual, interdecadal). The SH atmospheric circulation exhibits significant patterns of interannual to interdecadal variations (Garreaud and Battisti 1999; Kidson 1999 and references therein). Increased understanding of the relationships between the low-frequency variations and the WRs is necessary to better establish the nature and mechanisms of the large-scale interaction in the SH and their regional impacts over southern South America. In this sense, an important issue is to determine whether specific WRs tend to occur at particular phases of El Niño-Southern Oscillation cycle (ENSO) and, also, to investigate changes in the frequency of regimes over the last decades.

The study is organised as follows. Section 2 describes the dataset and statistical methodology applied. Then we proceed in Sect. 3 to the classification of the WRs, their spatial patterns and temporal evolution. Linkage between the obtained WRs and local climates over Argentina is analysed in Sect. 4. Interannual and interdecadal variability of WRs frequencies are presented in Sect. 5 and a summary and concluding remarks are found in Sect. 6.

2 Data and methodology

In order to perform the classification of WRs we used 34 years of the NCAR/NCEP re-analysis data set comprising daily averages of 500 hPa geopotential heights for the period 1966–1999 in a

$2.5^\circ \times 2.5^\circ$ latitude–longitude grid (Kalnay et al. 1996). They represent one of the most complete, physically consistent atmospheric datasets and have been used for a wide range of studies in the SH. Though the reanalyses data assimilation system remained fixed, it could be affected by changes in the observing system, particularly due to the lack of satellite data over the Southern Ocean prior to 1979. Discussions about its quality on a monthly mean and daily basis over the SH can be found in Garreaud and Battisti (1999), Simmonds and Keay (2000), Renwick and Revell (1999), Kistler et al. (2001), Carril and Navarra (2001). In a previous study (Solman and Menéndez 2002) the stability of some synoptic-scale patterns has been demonstrated and thus we can consider this dataset to be reasonably homogeneous for the study of the large-scale circulation during the period.

We considered SH winter season, as the 92-days period from 1 June to 31 August. The domain chosen extends from 120°W to 20°W and from 85°S to 20°S , and it was defined to study the large-scale circulation patterns that affect the South eastern Pacific – South America – South Atlantic sector. It includes 1025 gridpoints. Although the data contain $92 \times 34 = 3128$ maps these are not statistically independent of each other. For statistical purposes, based on autocorrelation statistics, we have considered only 300 degrees of freedom.

No prior classification into weather regimes using such a long database has been made for southern South America. However, it should be mentioned that Compagnucci et al. (1985) discussed different methodologies for classification of synoptic situations for this region and Compagnucci and Salles (1997) characterised the main synoptic patterns over southern South America by means of a principal component analysis of observed daily sea-level pressure for the period 1972–1983.

In order to link the WRs with the regional climate we have used temperature and precipitation station data. The regional datasets consist of daily precipitation station data for central and northern Argentina (although a few Brazilian stations were also included) from a database of the Department of Atmospheric and Oceanic Sciences (University of Buenos Aires) and daily temperature maxima and minima from 77 stations within Argentina, provided by the National Meteorological Service of Argentina and compiled by Rusticucci and Barrucand (2002), for the period 1959–1998. Daily averages of temperature are formed from the daily maxima and minima.

The identification of WRs has been performed following the clustering algorithm from MVL, named the K-means clustering method, which is a partitioning algorithm known as the dynamic cluster method based on recurrent patterns (ANAXV package provided by the Laboratoire de Météorologie Dynamique/CNRS, France). This methodology has been used in several studies to classify large-scale circulation patterns in the Northern Hemisphere (e.g. Robertson and Ghil 1999; Kageyama et al. 1999; Plaut and Simonnet 2001). A complete description of the method used here can be found in MVL and only a brief summary will be presented. We first subtract the climatological average from the data and work on the anomalies from this average, as in Kageyama et al. (1999). No prior time filtering is performed. After removing the grand mean to define the anomalies, an EOF analysis is first performed in order to reduce the dimension of the data set. The projections on the eight leading eigenvectors are retained which explain 83% of the variance. This procedure represents a spatial filtering which has the advantage of compressing the information along directions in the phase space that retain most of the variability. The cluster analysis is then performed in this reduced EOF space. Assuming a predetermined number of clusters, the algorithm starts from a set of as many random seeds as the chosen number of clusters and finds a partition of the entire dataset that minimises the sum of variances within each cluster. In order to find the optimal number of clusters the clustering algorithm is run 50 times from different initial sets of random seeds and a classifiability index is calculated as the average of pattern correlation among the members of each partition. The higher the classifiability index, the more similar the members of each partition are and, then, the more robust the classification is. This algorithm finds the optimal partition of

the whole data set and forces each map to fall into one of the identified clusters. In order to set significance limits for this index this is compared to the results from a first order Markov process having the same covariance matrices at lags 0 and 1 as the initial data set. The classifiability index is then calculated for 100 random samples and the upper and lower bound of confidence are assigned to the 10th highest and 10th lowest values of these indices. Then, the classifiability index of the true data set is compared with these bounds and the optimal number of clusters is defined as the one in which the classifiability index of the true data set is higher than that of the red noise model (MVL).

3 Weather regimes

3.1 Spatial patterns

Figure 1 shows the classifiability index as a function of the number of clusters, k , together with confidence limits of this index. The best choice for the number of clusters is the one for which the classifiability index is significantly higher than for the red noise model. Five clusters are found to be the most significant classification for the domain analysed. We performed several partitions modifying slightly the size of the window and found the same number of clusters arising as significant with the same spatial patterns for each weather regime. Thus, we concluded that the results shown are robust, independently of the size of the spatial domain.

We focus now on the spatial patterns of the WRs. Figure 2 displays the composite of the 500 hPa anomalies for each cluster. This figure includes the frequency of occurrence (as a percentage) in each class. As discussed by Plaut and Simonnet (2001), the cluster central patterns are not strictly weather regimes, in terms of being synoptic-scale patterns, rather, they represent the most recurrent and the more persistent anomalies in a given domain. This is because the clustering methodology is not able to capture the rapidly travelling anomalies and,

thus, they represent frequencies lower than those on the synoptic-scale. Nevertheless, as accepted in the literature, we will refer to these patterns as WRs.

WR 1 is characterised by a positive anomaly over the southeastern Pacific Ocean and a negative anomaly over the southwestern Atlantic Ocean, inducing an anomaly in the advection that intensifies cold air advection over southern South America. WR 2, is characterised by a negative anomaly over the southeastern Pacific Ocean and a positive anomaly east of the Antarctic Peninsula, which resembles a blocking episode over the south Atlantic Ocean, as described in Trenberth and Mo (1985). This pattern induces anomalous northeasterly flow and consequently a weakening of the westerlies over the southern tip of South America. In WR 3, a positive anomaly is positioned over the Bellingshausen Sea (90°W), surrounded by negative anomalies over the mid-latitudes Atlantic and Pacific oceans. This pattern induces southeasterly flow anomalies and intensifies cold-air advection over southern South America. WR 4 presents a cyclonic anomaly over the Bellingshausen Sea and a positive one over the mid-latitudes Atlantic Ocean, inducing enhanced mid-latitude westerlies over Patagonia, and northeasterlies over much of subtropical latitudes of South America. Finally, WR 5 is characterised by a positive centre to the west of the southern tip of South America and a trough over the Atlantic Ocean, inducing a weakening of the westerlies over subtropical latitudes, strengthening the sub-polar jet and intensifying cold-air advection over southern South-America. Concerning the vertical structure of the regimes, we performed composites of geopotential height anomalies for each WR at 1000, 850 and 300 hPa (not shown) and we found that the structures are predominantly barotropic.

The patterns detected from the cluster analysis, with exception of WR 5, resemble PSA-like patterns found in previous studies of intraseasonal variability of the SH. WR 1 and WR 2 compare closely with PSA 1 mode for negative and positive phases, respectively, and WR 3 and WR 4, compare with PSA 2 mode negative and positive phases, respectively, constructed by Mo and Higgins (1998). Moreover, WR 1 and WR 3 resemble the typical composite for the warm phase of ENSO with a blocking high over the southeastern Pacific Ocean, and WR 2 agrees with classic composite for cold events (e.g. Garreaud and Batisti 1999).

3.2 Persistence

Analysis of persistence of the weather regimes found and transition among them is worth studying in terms of the linkage with local weather conditions, mainly over the continental area. In particular, persistence of anomalous conditions in local weather could be inferred from WRs persistence and their transitions. We will turn to this point after analysing the composites of local temperature and precipitation for each WR.

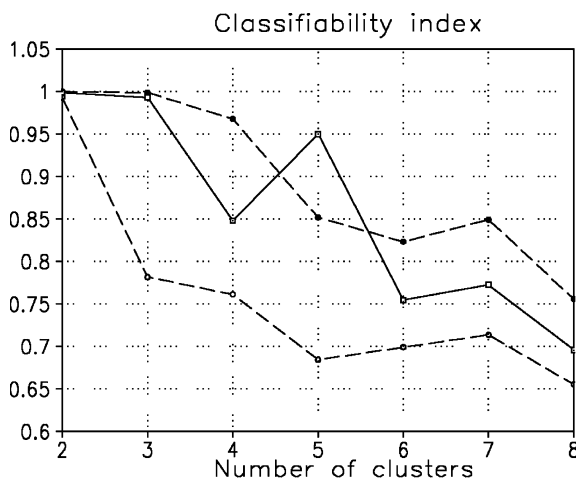


Fig. 1 Classifiability index as a function of the number of clusters k (solid line). Dashed lines represent the upper and lower bounds (90% and 10%, respectively) of the classifiability index calculated from a red-noise model

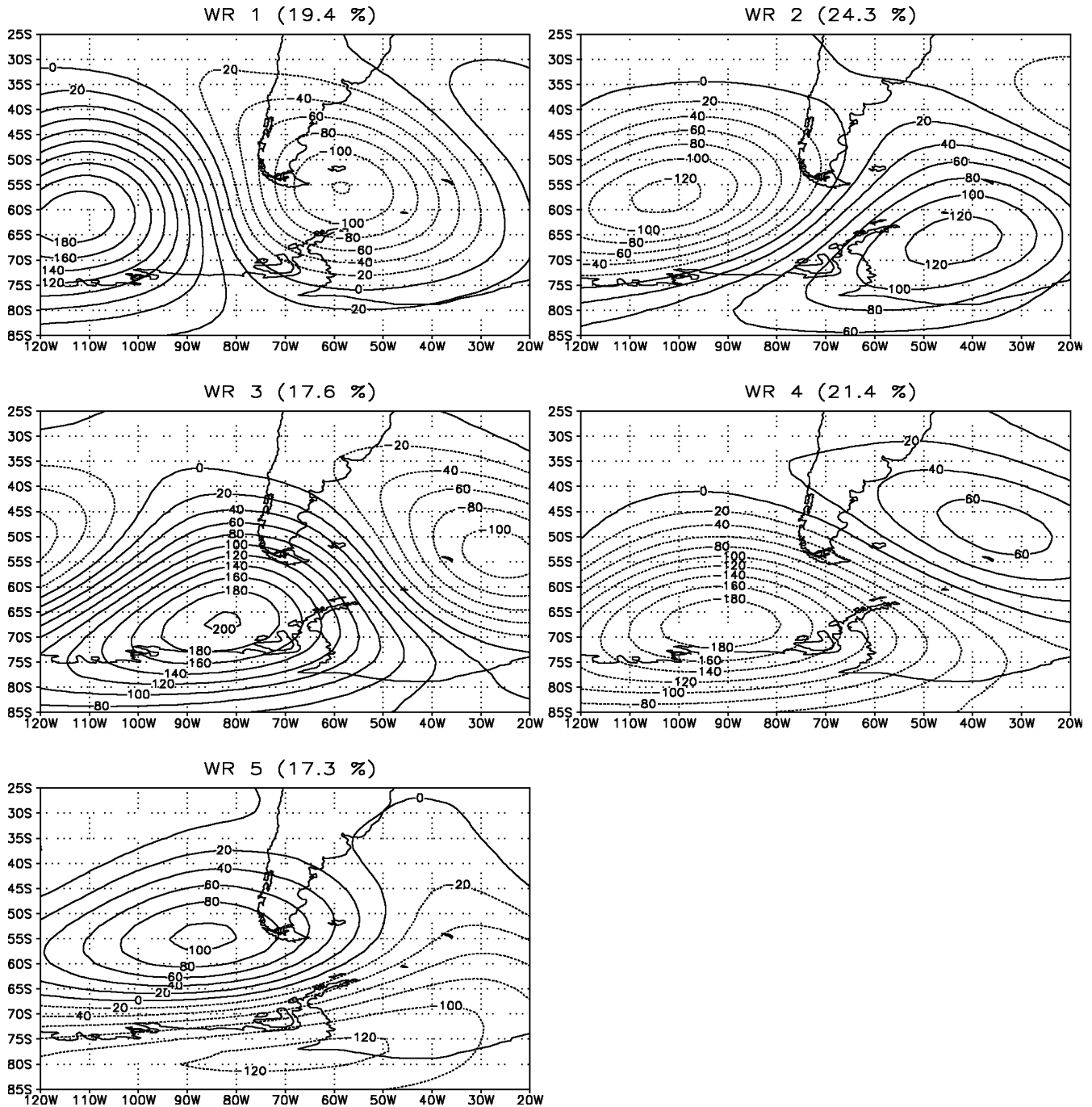


Fig. 2 Composite maps of 500 hPa anomalies for the five weather regimes: a WR 1; b WR 2; c WR 3; d WR 4 and e WR 5. In Percentage of days for each WR indicated in parenthesis

Table 1 summarises the characteristics of each regime: average duration, number of events, number of days belonging to each WR and the percentage (number) of events with given duration. Figure 3 shows in graphical format persistence characteristics of each regime.

Average duration of events range from three to five days, nevertheless, it is interesting to note that WR 2 accounts for the largest duration and the largest number of events that last more than five days (42.4%). In this

case, this weather pattern is representative of blocking over the southeastern Atlantic Ocean. WR 5 is the shortest-lived one and accounts for the largest number of short events, with a duration of 1 to 4 days (80.3%). This regime represents short-lived transient ridges over the southwestern Pacific Ocean and is in agreement with the secondary maximum frequency of short-lived positive anomalies shown by Trenberth and Mo (1985). This is also reflected in the composites of meridional wind anomaly variance (not shown) for WR 5, which resem-

Table 1 Characteristics of the WRs identified. The columns list the mean duration (in days), the number of events (N_e), the number of days (N_d) and the percentage (number) of events of a given duration in days

WR	Mean duration (days)	Number of events (N_e)	Number of days (N_d)	Percentage of events with duration T days (number of events)		
				$T \leq 4$	$5 \leq T \leq 9$	$T \geq 10$
1	3.9	157	609	70 (110)	22.3 (35)	7.6 (12)
2	4.6	163	759	57.7 (94)	35 (57)	7.4 (12)
3	4.1	135	551	63 (85)	31.1 (42)	6 (8)
4	4.4	151	669	62.2 (94)	26.5 (40)	11.2 (17)
5	3.2	168	540	80.3 (135)	14.9 (25)	4.8 (8)

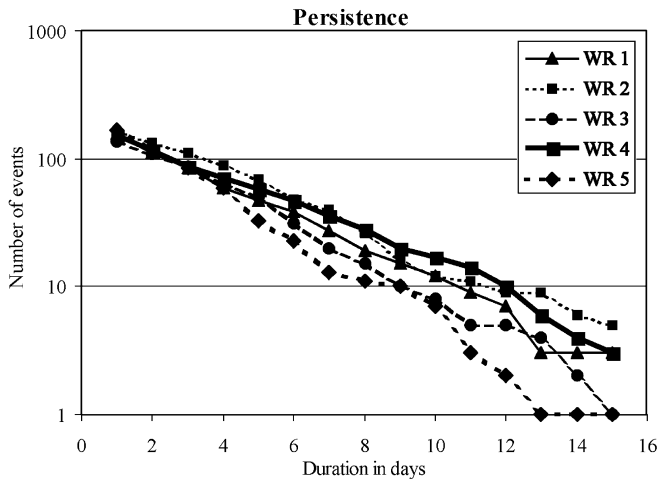


Fig. 3 Number of events versus duration in days for the five weather regimes

bles the climatology of the main tracks of transient disturbances (storm tracks).

In Fig. 3 the log-linear plot of number of events vs. duration for each WR reflects the fact that WR 2 and WR 4 tend to persist longer and for WR 5 the slope of the curve is larger, particularly after day 4. In terms of the interpretation in Dole and Gordon (1983), the slope of the curves represent the probability of persistence another day, after lasting n days, with shallower slopes indicating a higher probability of continuation. The slope for WR 5 becomes larger for longer duration, while the opposite occurs for the other WRs.

3.3 Transitions

Transitions between regimes can be quantified as the number of passages from one weather regime to another. In this work we have studied the transitions between events corresponding to two different regimes (M and N , with $M, N = 1$ to 5). They were calculated as the number of times that a transition occurs from event M to event N divided by the total number of the events M . We only considered the cases in which both events have durations longer than four days. However, it should be mentioned that we have also quantified the transitions taking into account all the events, no matter their duration, with similar results. Table 2 displays, as a percentage, the transitions obtained. We also computed the statistical

Table 2 Percentage of transitions between regimes for events longer than 4 days. Significant transitions at 90% confidence level are indicated by an asterisk

To From	WR 1	WR 2	WR 3	WR 4	WR 5
WR 1	–	7	60*	4	29
WR 2	36	–	12	39	13
WR 3	17	66*	–	3	14
WR 4	35	26	0	–	39
WR 5	15	9	14	62*	–

significance of the transitions by reshuffling the observed events 1000 times, so having 1000 random time series, as was proposed in Kimoto and Ghil (1993). Tables similar to Table 2 were constructed for each random time series and we considered the more likely transitions to be those that are exceeded by less than 100 simulated ones. Thus, the transition is considered more likely at a 90% confidence level. In Table 2 significant transitions at a 90% level are indicated with an asterisk.

The results in Table 2 suggest that the more likely transitions follow the sequence indicated in Fig. 4. Preferred transitions from WR1 to WR 3 then to WR 2 then to WR 4 and back to WR 1 and also from WR 1 to WR 3 then to WR 2 and back to WR 1 denote a progression of the Rossby wave-like eastern propagation. This agrees with the findings by Mo and Higgins (1998).

A rough estimate of the longer oscillation, by summing up the average durations listed in Table 1, is about 17 days. This agrees with the intraseasonal oscillation with period of about 18 days found for the fifth and sixth modes for both PSA in Mo and Higgins (1998) (their Table I). However, we should emphasise that this complete oscillation is not always realised in any given winter, often only a few segments may appear consecutively.

Another interesting point to discuss is how initiations and terminations of WRs take place and how long before the initiation and after the termination of each WR it is possible to identify preferred precursors and successors, respectively. We first computed time lagged correlation coefficients between time series built with the first day or onset (alternatively last day or breakup) of an event for each WR, and the corresponding time series for each WR. A summary of the results are displayed in Table 3 which shows the lags for which correlation coefficients are significantly different from zero (95%).

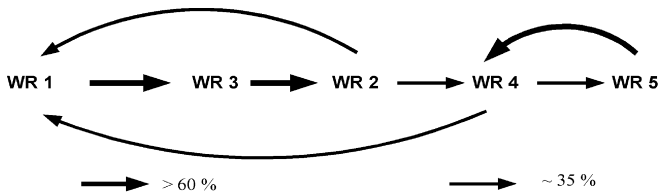


Fig. 4 Preferred transitions between WRs. The *thickness of the arrow* indicates the recurrence of the transition

Table 3 Days before onset and after breaks for which time series of onsets and breakups are significantly correlated with time series of occurrence of WR

	Onsets		Breakups	
	Time lag (days)	WR before onset	Time lag (days)	WR after breakup
WR 1	-2 to -1	WR 2	+1 to +6	WR 3
	-2 to -1	WR 4	+1 to +3	WR 5
WR 2	-5 to -1	WR 3	+1 to +2	WR 1
			+1 to +2	WR 4
WR 3	-6 to -1	WR 1	+1 to +5	WR 2
WR 4	-2 to -1	WR 2	+1 to +2	WR 1
	-4 to -1	WR 5	+1 to +4	WR 5
WR 5	-2 to -1	WR 1	+1 to +3	WR 4
	-5 to -1	WR 4		

The results in Table 3 are consistent with those shown in Table 2, but additional information about the time lag before and after the occurrence of each WR (i.e. preferred precursor and successor, respectively) can be now identified. Those WR with only one preferred precursor or successor are easier to identify.

Time lagged composites of 500 hPa anomalies for days before onset (negative lags) and days after breakup (positive lags) have been performed for each WR. Figure 5 shows the composite for days before onset (lag -2) and days after break (lag +2 and +4) of WR1. It is preceded by a small negative anomaly centre in the southwest Pacific that resembles the pattern for WR 2 or WR 4. After the breakup, the negative anomaly centre with a positive centre upstream are shifted to the western Atlantic, resembling WR 3 pattern. The overall sequence of WR 1 composites suggests an eastward travelling wave train. The composites of days before onset (lag -4 and -2) and days after breakup (lag +2) for WR 2 in Fig. 6 suggest again an eastward progression of a wave train, being the composites before onset comparable with WR 3, and after breakup, a negative centre positioned over the southern tip of South America and a positive centre downstream, which may be related to either WR 1 or WR 4.

Figure 7, which displays the composites of days before onset (lags -4 and -2) and days after breakup (lag +2) for WR 3, supports the preferred transition discussed. Days before onset are dominated by a west-east dipole pattern that travels eastward, resembling WR 1. Days after breakups are characterised by a positive anomaly upstream the negative centre which has shifted

towards the Atlantic, in agreement with the pattern for WR 2. Composites of days before onset and days after breakup for WR 4 are less clear due to the fact that different patterns may cancel each other. For instance, Fig. 8 displays the composite of days before onset at lag -2, showing a positive anomaly over southern South America and a negative centre over the Antarctic coast in the Pacific Ocean, reminiscent of the WR 5 pattern. After the breakup, for lags +2 and +4, the WR 5 pattern is easy to identify.

With respect to days before onset for WR 5, Fig. 9a shows a positive anomaly near 115°W. Examination of other negative lags (not shown) suggests that this is a migratory positive anomaly propagating eastward over the mid-latitudes of the South Pacific (Trenberth and Mo 1985). After the breakup, the centre of positive anomaly is further strengthened and negative anomalies are established downstream. At lag +4 the positive anomaly continues propagating eastward, with a negative anomaly upstream. Resemblance with WR 4 is evident at positive lags.

The preferred transitions discussed are seen in both the days before onset and the days after break of the regimes analysed. Moreover, the spatial patterns shown suggest the progression of a Rossby wave-like pattern propagating towards the east as the main fingerprint of large-scale patterns over the south Pacific – south Atlantic oceans.

4 Weather regimes and local climate

One of the main interests of this study relies on the influence of the most recurrent large-scale patterns on local climate. Furthermore, the analysis of persistence and preferred transitions among WRs may induce to sustained occurrence of anomalous local conditions. A few descriptions concerning some individual regimes and their effects on local climate over Argentina have been previously published in the regional literature. For example, Malaka and Núñez (1980) on the effect of blocks on regional weather and Berbery and Alfaro Lozano (1991) on persistent anomalies and their effect on precipitation and temperature in Argentina.

4.1 Temperature

The local climate conditions associated with each WR are first described by calculating the composites of temperature anomalies for a subset of dates for which a given WR occurs. We computed the composites for 77 Argentine station data observed temperatures (more details on datasets can be found in Sect. 2). Significance of the composite anomalies has been tested by means of a pointwise *t*-test with a number of degrees of freedom taken as the number of events minus one. It is worth mentioning, however, that this assumes complete independence of each event. Nevertheless, lower

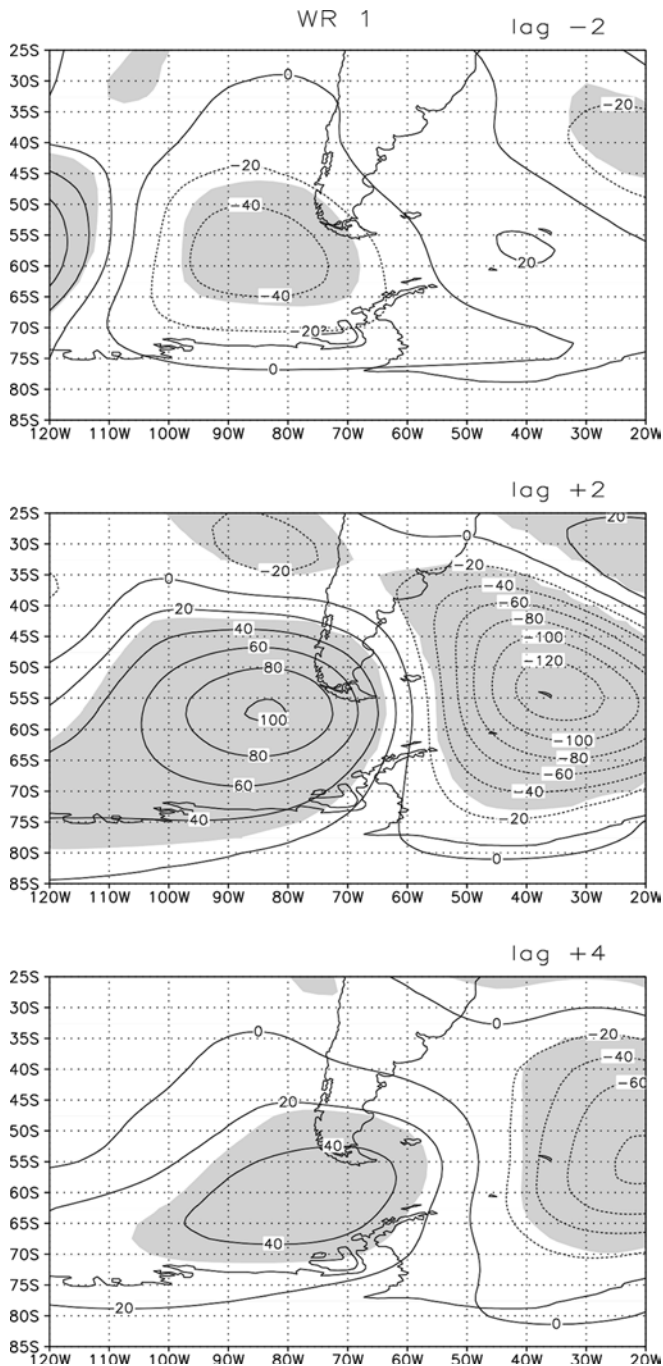


Fig. 5 Composite maps of 500 hPa anomalies of WR 1 for onsets at **a** day -2 and breakups at **b** day $+2$ and **c** $+4$. Shaded areas represent statistically significant anomalies at a 95% level by a pointwise t -test with a number of degrees of freedom taken as the number of events minus one

frequency oscillations may favour the occurrence of certain regimes and this may reduce the number of degrees of freedom. Figure 10 displays the composites for the five regimes. The relationship between 500 hPa anomalies and temperature anomalies stems primarily from the result of air advection, considering that the WRs have a predominantly barotropic structure. The

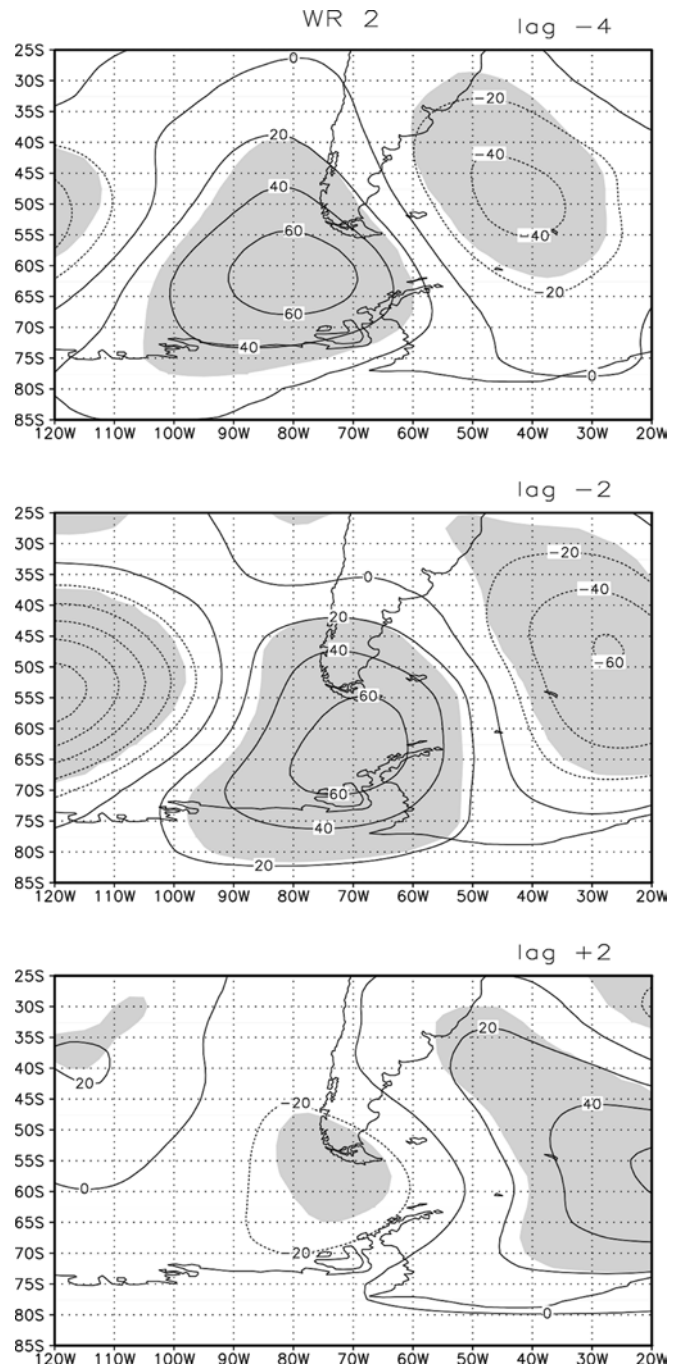


Fig. 6 Same as Fig. 4 for WR 2 at **a** days -4 and **b** -2 for onsets, respectively and at **c** day $+2$ for breakups

largest negative anomalies are found for WR 1 (over southern Argentina) and WR 3 and the largest positive temperature anomalies for WR 1 (over northern Argentina) and WR 4. Negative anomalies over southern Argentina for WR 1 can be expected due to the presence of a strong cyclonic anomaly located over south-western Atlantic Ocean, which favours cold air advection from high latitudes. For WR 3 the positive anomaly over the Bellinghousen Sea favours strong cold air advection over almost all stations. The strongest preferred transition

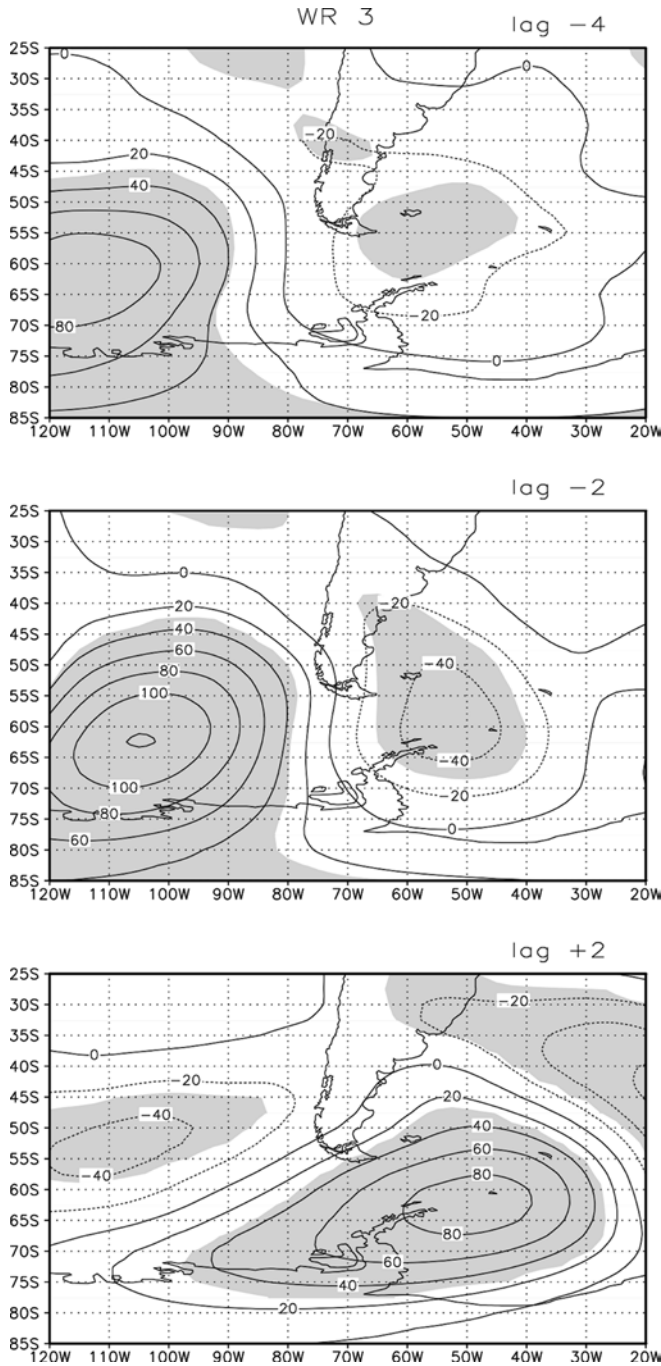


Fig. 7a-c Same as Fig. 6 for WR 3

from WR 1 to WR 3 gives rise to sustained cold conditions over southern Argentina. The following preferred transition from WR 3 to WR 2 tends to induce sustained cold anomalies over the northern part of the country. Positive temperature anomalies over Argentina for WR 4 can be expected due to advection from the northeast, associated with the presence of the positive anomaly over the Atlantic Ocean. WR 5 induces significant anomalously cold conditions all over the country. It is worth noting that many transitions from

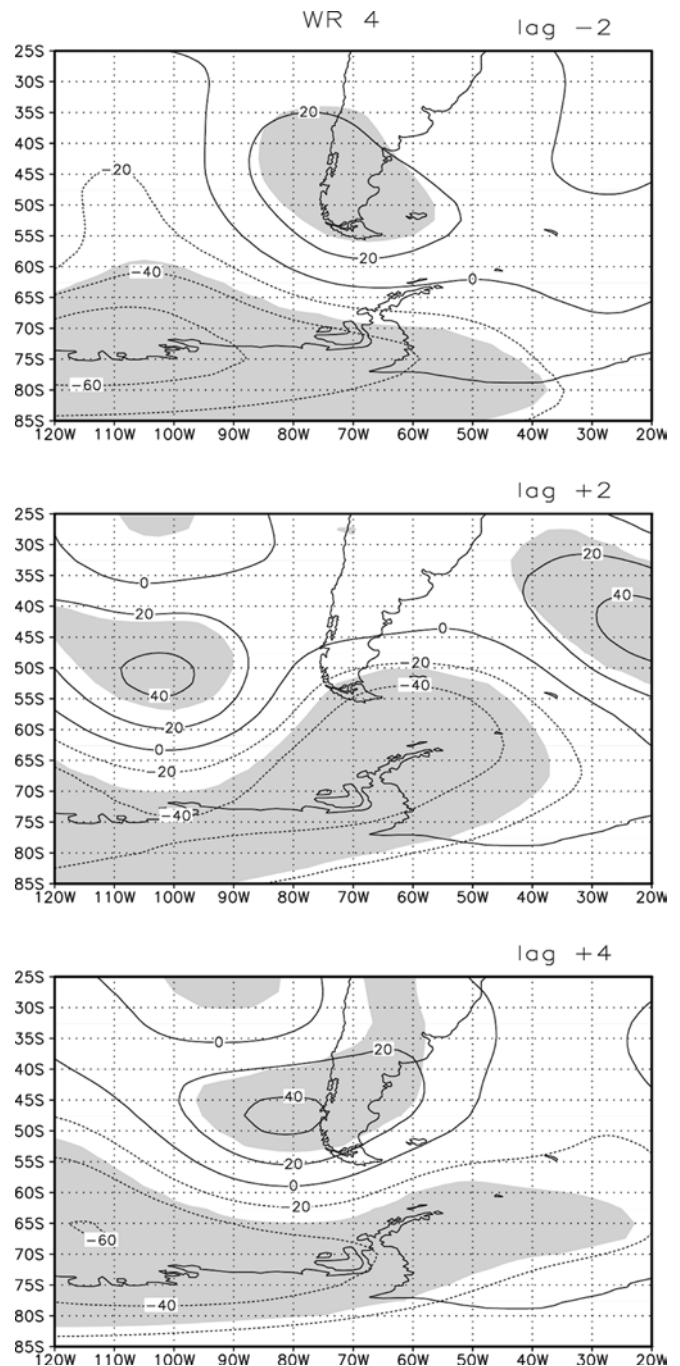


Fig. 8a-c Same as Fig. 5 for WR 4

one regime to another tend to cancel their impact over local temperature anomalies (e.g. from WR 5 to WR 4).

4.2 Precipitation

The influence of WRs on precipitation frequency is analysed in this section. The regional dataset consists of observed daily precipitation totals for seven regions within central and northern Argentina. The geographical

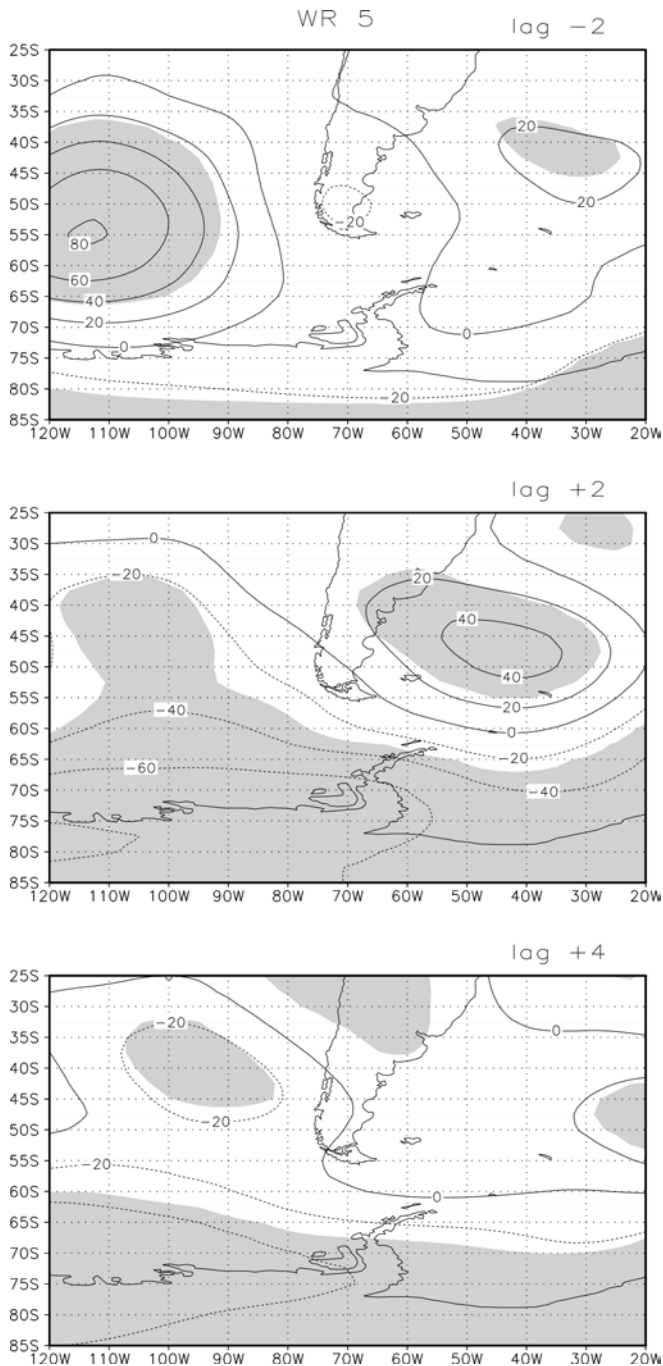


Fig. 9a-c Same as Fig. 5 for WR 5

locations of the stations and regions are given in Fig. 11. The annual cycle of precipitation and the mean rainfall amount for winter at each station were considered in order to define the regions. Actually, the minimum in the annual march of precipitation is reached in winter for all the regions with relatively dry conditions over central and western Argentina (Grimm et al. 2000). Each regional time series consists of a daily average over five to 13 stations. Not all the stations report information over the entire period considered. Table 4 displays for each

region the total number of data over the entire period and the wintertime mean climatology. This daily dataset helps to quantify the interregional variability across Argentina north of 40°S between 1966 and 1999.

Two kinds of comparisons were performed: the first associates with the local percentage of ‘rainy’ days (daily average of rainfall amounts greater than 0.5 mm/d) and the second to ‘intense precipitation’ days (defined here as rainfall amounts greater than 5% of the winter climatology). The changes (in %) in rainy day frequency for each WR and for the different regions as compared to local climatic average are presented in Table 5. Similarly, Table 6 shows the changes in intense precipitation day frequency. The significance of results is again estimated using a simple reshuffling Monte Carlo procedure with 1000 random shuffles.

About a half of the entries in Table 5 suggests rainy days that are significantly more or less frequent than for the whole dataset at the 95% or 99% level. The regimes also tend to show frequency anomalies of different signs by region. For example, WR 1 is significantly wetter for regions A and C and significantly drier for region E. The most significant departure from climatology is found for WR 3, with wetter conditions over all the regions. This may be associated with the presence of persistent anti-cyclones southwest of the southern tip of South America, which may divert depressions to the north. In contrast, WR 4 tends to induce significantly drier conditions especially over the eastern part of the country, consistent with positive anomalies of geopotential height downstream this region. Similarly, WR 2 also shows a reduced frequency of rainy days over most of the country, especially over the three western regions (D, E and F). These same three regions experience the “reverse” conditions for WR 5, with significantly wetter days.

Changes in the frequency of intense precipitation events are qualitatively similar to those described for rainy days, but tend to be less statistically significant (17/35 and 12/35 entries are significant in Tables 5 and 6 respectively). Major increases in the occurrence of intense rain (at the 99% level of significance) are found in region A for WR 1, region D for WR 3 and near the Andes Mountains (regions E and F) for WR 5. The only decrease at the 99% level of significance is found in region D for WR1. Note that for region G all the regimes lead to changes in the frequency that are not statistically significant, for both kinds of comparison (rainy days and intense precipitation days). Finally, it is important to remark that the chances of persistent rainy conditions for region C growth considering the likely transition from WR 1 to WR 3, whereas sustained dry conditions are expected for region A once WR 5 and its likely transition to WR 4 are established.

The temperature and precipitation anomaly patterns for each WR from NCEP reanalyses (not shown) are in general consistent with the features obtained from station data. The results suggest that at least a significant proportion of the anomalies for a given period are very

likely to originate in anomalous WR frequencies. In this sense, the WR approach is advantageous in order to coherently describe the local climate deviation from average.

5 Interannual and interdecadal variations

The influence of sea surface temperature (SST) anomalies in the equatorial Pacific in the SH circulation has been largely explored. Numerous authors described ENSO teleconnections over parts of the SH (e.g. Mo and White 1985; Karoly 1989; Rutllant and Fuenzalida 1991; Ambrizzi 1994; Mo and Higgins 1998; Garreaud and Battisti 1999). Its effect in inducing circulation anomalies over subtropical latitudes may be viewed as the Rossby wave response to thermal forcing. In this context, the well-known PSA pattern is the most important anomalous circulation induced by thermal forcing in the equatorial Pacific that affects southern South America. For example, an important signature related to ENSO events is the predisposition toward blocking southwest of the southern tip of South America during warm events, and vice versa during cold events (Rutllant and Fuenzalida 1991).

In order to quantify the change in regime frequency for warm and cold phases of the ENSO cycle, monthly mean sea surface temperature (SST) anomalies in El Niño 3 region from NCEP reanalysis were used. Following Solman and Menéndez (2002), a subset of 19 and 20 months corresponding to warm and cold phases, respectively, were built and the weather regime frequencies were calculated for each subset. Figure 12 illustrates the frequency (as a percentage) of each WR as the number of days belonging to each regime relative to the total number of days corresponding to warm and cold phases of the ENSO cycle. The asterisks denote the 95% significance level, based on 1000 random reshuffles. Double asterisks denote significance at a 99% confidence level. The frequency of the WRs for the full period has been included in the figure in order to highlight the changes for the extreme ENSO phases. The most significant changes in frequency arise for WR 1 and WR 2. WR 1 becomes more frequent during El Niño and less frequent during La Niña and WR 2 is more prevalent for La Niña and less prevalent for El Niño. Moreover, significant frequency changes are also found for WR3 (for warm events) and WR5 (for cold events). The other regimes do not show significant change in frequency of occurrence under La Niña or El Niño conditions. The significant increase of frequency of WR 1 and WR 3 for El Niño is consistent with the composite anomaly of 500 hPa geopotential field for El Niño years (Karoly 1989; Grimm et al. 2000; Garreaud and Battisti 1999) showing an anticyclonic anomaly over the southeast Pacific, inducing the typical blocking episodes to the west of South America and a negative anomaly over the southwestern Atlantic. The reverse situation is a common feature for

La Niña events, consistent with the increased frequency of WR 2.

Several studies of the Southern Hemisphere circulation report evidences of considerable variability on decadal and longer time scales (Hurrell and van Loon 1994; Burnett and McNicoll 2000). A considerable change in the SH circulation during the 1980s has been shown to be related to a weakening in the semi-annual oscillation. This weakening is thought to reflect changes in the amplitude of the zonal wave number 3, a deepening of the subAntarctic trough, intensification of subtropical ridging and, in consequence, a strengthening of the westerlies and enhancement of cyclone activity (Chen and Yen 1997). Though the record used in this study is not long enough to show strong evidences of changes in the circulation pattern, some significant differences arise that seem to be related to a manifestation of this known interdecadal variability. Figure 13 shows the number of occurrences of each WR per winter, together with its 10-year running means. Note in particular a substantial decrease in the frequency of WR 2 during the 1970s and early 1980s, together with an increase in the frequency of occurrence of WR 4 and WR 5 during that period. Significant linear trends (at a 99% confidence level) have been obtained for the period up to 1984. These trends agree with the strengthening of mid-latitude ridging and deepening of the circumpolar trough in the southern Pacific in winter as shown by Chen and Yen (1997). Results are also consistent with the observed trends in the SH tropospheric circulation toward stronger westerly flow around Antarctica mentioned by Thompson and Solomon (2002).

6 Summary and conclusions

In this study we classified 34 years of NCEP reanalysis daily 500 hPa geopotential heights over the western South Pacific–eastern South Atlantic oceans, in order to identify the most recurrent large-scale patterns, referred to as weather regimes, by means of a dynamical clustering algorithm. We found that the optimal classification was into five regimes (WRs). The spatial structures of the first four WRs resemble the phases of the intra-seasonal variability patterns known as PSA (Mo and Higgins 1998; Ghil and Mo 1991). The fifth WR is associated with transient anticyclones over the southern Pacific, which are usually relatively short-lived features (Trenberth and Mo 1985). Although some asymmetries exist, by comparing WR 3 with WR 4, and to a lesser extent WR 2 with WR 1 and WR 5, to a first approximation recurrent positive and negative anomaly patterns for a given region can be described as opposite phases of the same basic patterns of low-frequency variability. Amplifications of the amplitude and persistence of these patterns can be related to either a regionally intensified zonal flow or blocking. Upstream of South America, WR 1 and WR 3 are associated with strong meridional flow linked with cold air outbreaks (and eventually with

Fig. 10 Composite of temperature anomaly for the five WRs in Fig. 2. Shaded areas represent statistically significant anomalies at a 95% level by a pointwise t -test with a number of degrees of freedom taken as the number of events minus one. Station data from Argentina are indicated by asterisks

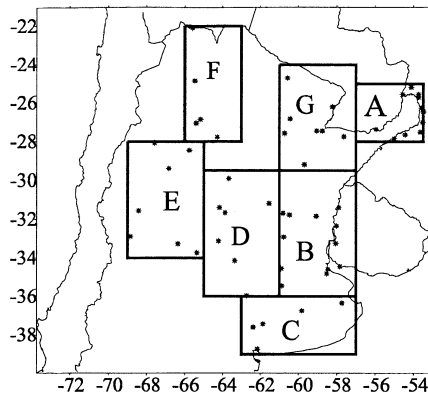
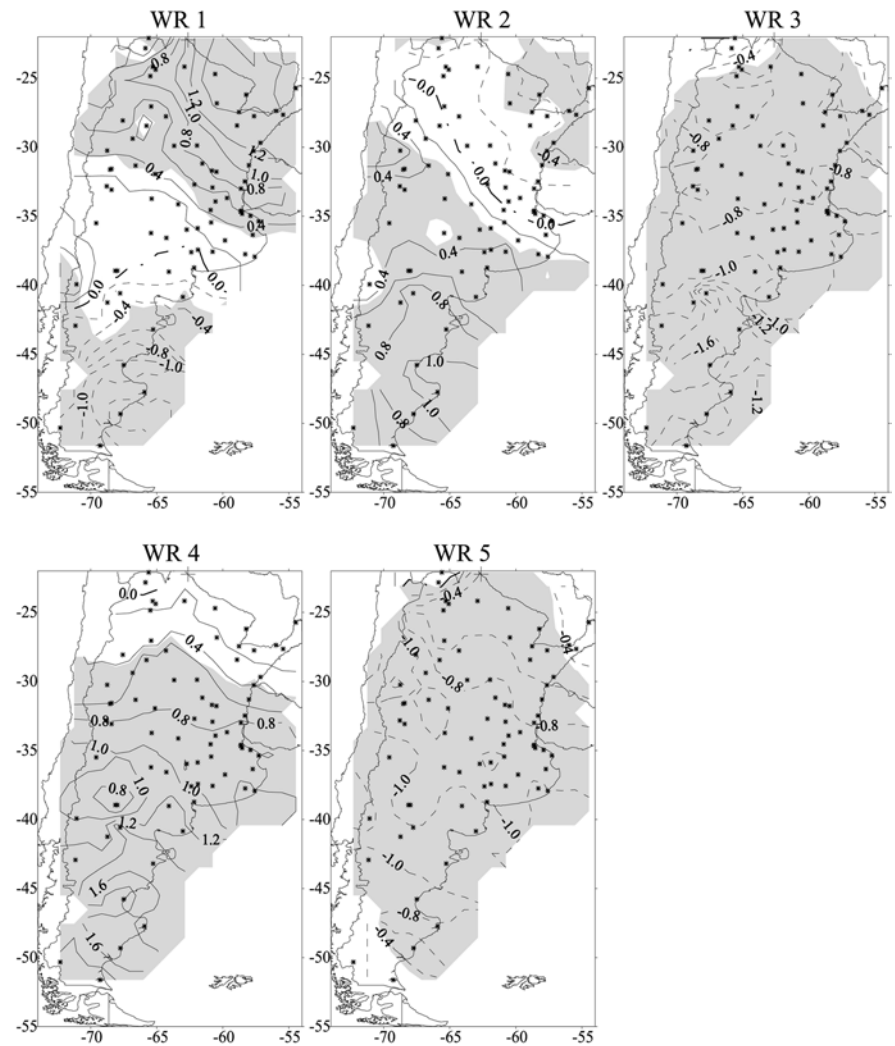


Fig. 11 Geographical location of stations and regions for the analysis of daily precipitation

blocking events), whereas WR 2, WR 4 and WR 5 are associated with an enhanced jet at subtropical, mid- and high latitudes, respectively.

We also described the preferred transitions between the patterns identified. We found that these transitions

may be interpreted as an eastward-propagating Rossby wave train. Thus, the chain of transitions between regimes is suggestive of the low frequency variability on intraseasonal time scales in the SH, mainly the PSA pattern. Though chains of preferred transitions have been suggested (from WR 1 to WR 3, then to WR 2, then to WR 4 and back to WR 1), they are not always completed within one winter. Infact, some segments of the circuit appear episodically. The notion of WRs and their preferred transitions suggests that the extratropical southern atmospheric circulation exhibits a chaotic but not totally random behaviour. The nonlinear feedback between ‘weather’ (i.e. the baroclinic transient waves) and the planetary low-frequency motions is the key phenomenon (Metz 1987) and helps to understand the occurrence of WRs and their preferred transitions. Even if we suggest this connection between low-frequency oscillation and recurrent circulation patterns, a comprehensive analysis of this relationship was beyond the our scope and will be the subject of future investigation.

The practical relevance in the classification of the large-scale circulation patterns into a few recurrent ones

Table 4 Total number of daily precipitation data for regions defined in Fig. 11 and June–July–August climatology

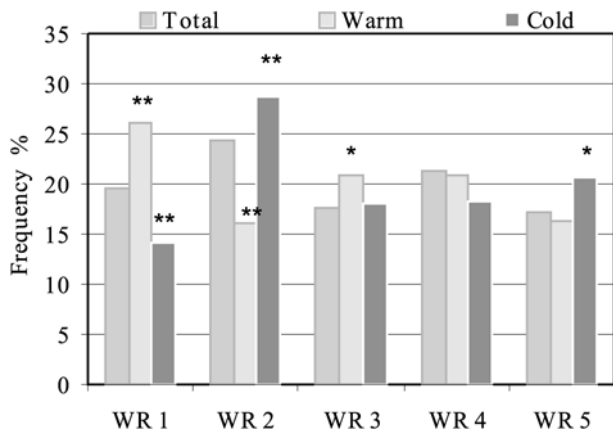
Region	Number of data	JJA climatology
A	27859	357.5
B	41857	141.8
C	16545	122.3
D	22111	48.9
E	20018	19.1
F	14365	64.3
G	28461	108.4

Table 5 Change in the frequency of wet days (precip. >0.5 mm/day). Significance at a 95% confidence level is indicated by an asterisk and significance at 99% confidence level is indicated by two asterisks

Region	WR 1	WR 2	WR 3	WR 4	WR 5
A	13.2**	-3.1	4.5	-10.3**	-2.4
B	0.3	7.0	13.2**	-13.5**	-7.0
C	18.3**	-4.6	18.7**	-26.1**	-0.9
D	-11.5	-19.2*	31.7**	-8.3	17.8*
E	-32.9**	-35.0**	38.1**	-3.1	51.3**
F	6.1	-26.8**	8.6*	4.1	16.9**
G	1.7	-4.6	9.3	-0.9	-3.9

Table 6 Change in the frequency of intense rainy days (precipitation >5% climatology JJA). Significance at 95% confidence level is indicated by an asterisk and significance at 99% confidence level is indicated by two asterisks

Region	WR 1	WR 2	WR 3	WR 4	WR 5
A	54.1**	-11.4	13.5	-25.2*	-27.6*
B	-21.3	4.0	22.7*	-11.5	9.6
C	24.7*	-8.0	18.5	-20.6	-10.0
D	-43.6**	-25.3	40.4**	23.3	14.6
E	-27.6*	-39.2*	34.6*	-10.1	63.4**
F	-29.3	-28.2	19.8	-18.5	75.4**
G	5.5	-13.5	3.9	16.9	-12.1

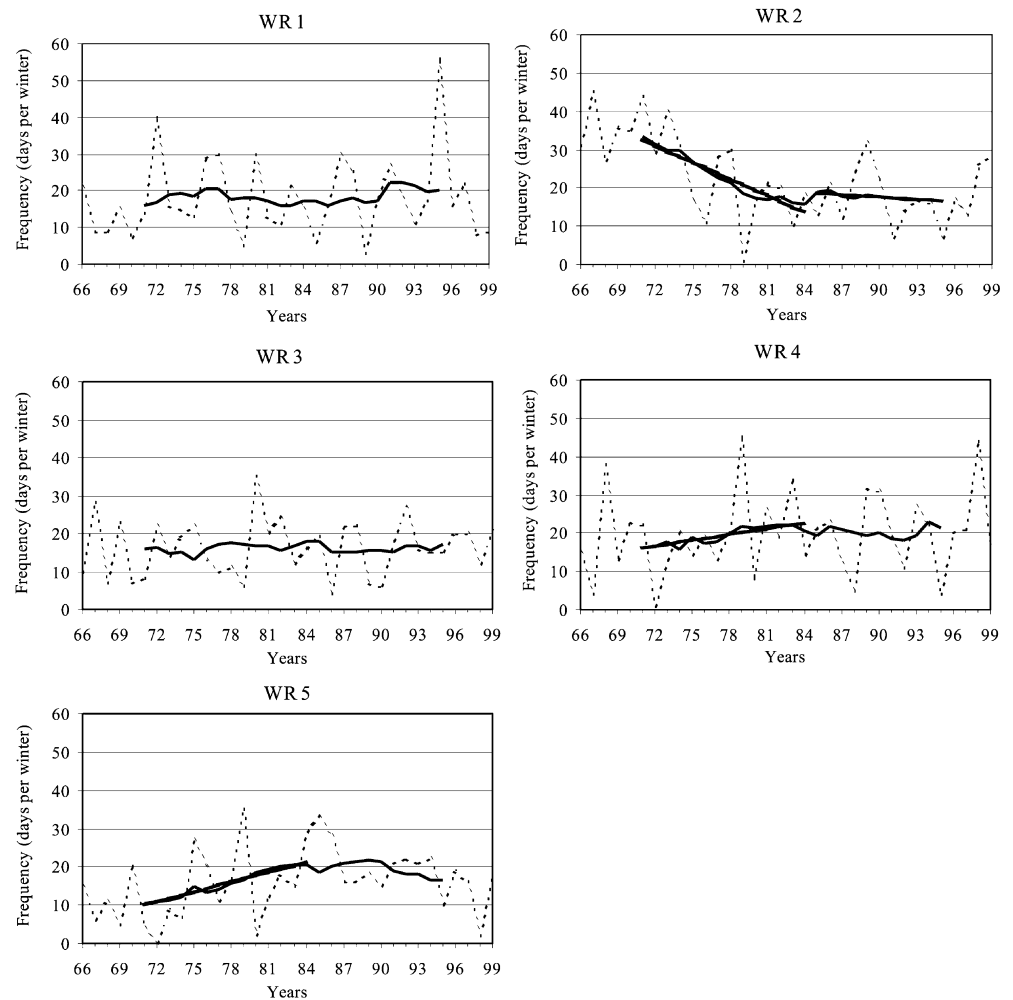
**Fig. 12** Regime frequency as a percentage (number of days of each WR/total number of days) for warm and cold phases of ENSO cycle. The total frequency of each WR is included for reference. Significance at 95% confidence level is marked with an asterisk. Double asterisks indicate significance at 99% level

lies in its impact on local weather (traditionally characterised by temperature and precipitation). The regimes organise synoptic activity and are accompanied by shifts in the location of the major storm tracks in the region. Moreover, transitions between regimes can have an enhanced influence particularly if transitions induce sustained anomalous conditions on local weather. We focused on the influence of WRs on surface weather elements over Argentina. Daily precipitation data unfortunately were only available north of about 40°S, while daily temperature data were available for the whole country.

The impact of WRs on local climate was analysed. Over the Patagonian region, WR 1, WR 3 and WR 5 induce cold weather, while WR 2 and WR 4 are associated with warm conditions. Over central and northern Argentina both temperature and precipitation were analysed. WR 1, characterised by an anomalous trough centred downstream the Drake Passage, tends to yield warm and wet conditions over the eastern part of the country and warm and dry conditions to the west. This regime may favour coastal activity associated with an enhanced storm track over the Atlantic, inducing an increase of the frequency of rainy days over southern Buenos Aires province (region C). WR 2, characterised by an anomalous trough over the SW Pacific and an anomalous ridge over the SE Atlantic, induces drier than normal weather over most of the region with cold conditions to the NE and warm conditions to the SW. WR 3 and WR 4 are connected with the most homogeneous anomalies in local weather (i.e. anomalies of the same sign all over the region). WR 3 is mostly cold and wet, while WR 4 tends to yield warm and dry weather (especially over eastern Argentina). The difference in temperature can be explained in terms of an anomalous ridge (trough) for WR 3 (WR 4) over the SE Pacific and a NW–SE anomalous trough (ridge) downstream, with strong advection of cold (warm) air from SE (NE). The contrast in the frequency of wet days can be associated with shifts in the storm track, for WR 3 it is deflected northward into subtropical South America, while for WR 4 the synoptic activity is enhanced over northern Patagonia. WR 5, characterised by a small amplitude anticyclonic anomaly to the west of the southern tip of South America and an anomalous ridge downstream, induces cold and relatively dry weather over eastern Argentina and cold and wet conditions to the west (note that this regime induces opposite weather compared to WR 1).

The influence of WRs on surface weather elements is even more considerable if the anomalous conditions are maintained through two consecutive regimes. Only some of the preferred transitions found induce statistically significant persistent anomalies in temperature or precipitation. Sustained cold anomalies were found associated with transitions from WR 1 to WR 3 and from WR 3 to WR 2 over southern and northern Argentina, respectively. Sustained rainy weather is likely to occur over southern Buenos Aires province once the former

Fig. 13 Number of occurrences of each WR per winter (*thin dashed line*), 10-year running means (*thick line*) and significant linear trend with 99% confidence (*thick line*)



transition is set up. On the other hand, persistent dry conditions tend to settle over northeastern Argentina when WR 5 is followed by WR 4.

Southern Hemisphere (SH) atmospheric circulation exhibits significant patterns of interannual to interdecadal time scales (Garreaud and Battisti 1999), which can modulate the WRs mainly through changes in the basic state. With this in mind we explored to what extent regime frequencies are influenced by interannual and interdecadal variability. We found that ENSO is characterised by anomalously high frequency of WR 1 and WR 3 during El Niño, and WR 2 during La Niña. To a smaller extent WR 5 is more frequent during La Niña. These results, in agreement with previous findings about tropical–extratropical interactions associated with ENSO (Mo and White 1985) suggest that the teleconnections associated with ENSO during winter can be interpreted as anomalous frequencies in the WRs over South America.

On interdecadal time scales, a significant decrease in WR 2 frequency and increase of WR 4 and WR 5 up to the early 1980s was found. These changes in the trend may be related to the observed interdecadal variability of the SH polar vortex and the Antarctic Circumpolar

Wave (Hurrell and van Loon 1994; Burnett and McNicoll 2000; Chen and Yen 1997). These trends are associated with modifications in the mean meridional transport of heat and momentum by atmospheric eddies. This would presumably affect the zonally symmetric mode of variability between the mid- and high latitudes, the semi-annual oscillation and sea ice around Antarctica, but these relationships and the mechanisms require further investigation. In particular, it is interesting to note that the variations in the frequencies of regimes 2, 4 and 5 during the 1970s and 1980s are consistent with the larger meridional geopotential height gradient and with an increase in the strength of the westerlies observed through that period (Burnett and McNicoll 2000).

Results here imply that part of the surface weather anomalies for a given period are very likely to originate in unusual regime frequencies. In this sense, the WR approach is advantageous in order to coherently describe the local climate deviation from average. It also can be useful as a downscaling tool, promising for climate variability or climate change studies. An important question arising is to what extent this analysis would be useful as a forecast tool. Our remarks reinforce the idea of using this knowledge as a complement that can help

to improve forecast beyond the synoptic time scale. In this sense, the forecast of sustained anomalous conditions is facilitated when a preferred transition occurs. As mentioned before, the regimes in the South American region are associated with particular phases of the main oscillations of the southern extratropics. As a consequence, in order to occur these regimes need a favourable large-scale environment. It should be remarked that since oscillations are the easiest sorts of phenomena to predict, the probability of occurrence of at least some regimes could be envisaged well in advance.

Acknowledgements This work was supported by ANPCyT Grant 7-6335, UBACYT Grant 01-X072, ECOS Grant A99U01 and IAI CRN 055. The authors are grateful to Drs. Isidoro Orlanski and Hervé LeTreut for their helpful comments and discussions on many topics of this study. Comments and suggestions by Dr. Hugo Berbery and an anonymous reviewer helped to improve the manuscript. We also thank Sebastien Conil and Bibiana Cerne for technical assistance. NCAR-NCEP reanalysis data were provided through the NOAA Climate Diagnostics Center. Station data were provided by Servicio Meteorológico Nacional (Argentina) and Dto. de Cs. de la Atmósfera y los Océanos (UBA).

References

- Ambrizzi T (1994) Rossby wave propagation on El Niño and La Niña non-zonal flows. *Rev Bras Meteor* 9: 54–65
- Berbery H, Alfaro Lozano L (1991) Características regionales de anomalías de alturas persistentes en los océanos Atlántico y Pacífico Sur. *Proc 6^{to} Congreso Argentino de Meteorología*, Buenos Aires, September 1991, pp 153–154
- Burnett AM, McNicoll AR (2000) Interannual variations in the Southern Hemisphere winter circumpolar vortex: relationships with the semiannual oscillation. *J Clim* 13: 991–999
- Carril AF, Navarra A (2001) Low-frequency variability of the Antarctic circumpolar wave. *Geo Res Lett* 28: 4623–4626
- Chen TC, Yen MC (1997) Interdecadal variation of the Southern Hemisphere circulation. *J Clim* 10: 805–812
- Compagnucci RH, Salles MA (1997) Surface pressure patterns during the year over southern South America. *Int J Climatol* 17: 635–653
- Compagnucci RH, Fornero L, Vargas WM (1985) Algunos métodos estadísticos para tipificación de situaciones sinópticas: Discusión metodológica. *Geoacta* 13: 43–55
- Dole RM, Gordon ND (1983) Persistent anomalies of the extratropical northern hemisphere wintertime circulation: geographical distribution and regional persistence characteristics. *Mon Weather Rev* 111: 1567–1586
- Garreaud RD, Battisti DS (1999) Interannual (ENSO) and interdecadal (ENSO-like) variability in the Southern Hemisphere tropospheric circulation. *J Clim* 12: 2113–2123
- Ghil M, Mo K (1991) Intraseasonal oscillations in the global atmosphere. Part II: Southern Hemisphere. *J Atmos Sci* 48: 780–790
- Grimm A, Barros V, Doyle M (2000) Climate variability in southern South America associated with El Niño and La Niña events. *J Clim* 13: 35–58
- Hurrell JW, van Loon H (1994) A modulation of the atmospheric annual cycle in the Southern Hemisphere. *Tellus* 46a: 325–338
- Kageyama M, D'Andrea F, Ramstein G, Valdes PJ (1999) Weather regimes in past climate atmospheric general circulation model simulations. *Clim Dyn* 15: 773–793
- Kalnay E and Co-authors (1996) The NCEP/NCAR 40-Year Reanalysis Project. *Bull Am Meteorol Soc* 77: 437–471
- Karoly DJ (1989) Southern Hemisphere circulation features associated with El Niño – Southern Oscillation events. *J Clim* 2: 1239–1252
- Kidson JW (1988) Interannual variations in the Southern Hemisphere circulation. *J Clim* 1: 1177–1198
- Kidson JW (1999) Principal modes of Southern Hemisphere low frequency variability obtained from NCEP/NCAR reanalyses. *J Clim* 12: 2808–2830
- Kiladis GN, Mo KC (1998) Interannual and intraseasonal variability in the Southern Hemisphere. In: Karoly DJ, et al. (eds) *Meteorology of the Southern Hemisphere*. Meteorological Monographs, AMS, Boston, pp 307–336
- Kimoto M, Ghil M (1993) Multiple flow regimes in the Northern Hemisphere winter. Part II: sectorial regimes and preferred transitions. *J Atmos Sci* 50: 2645–2673
- Kistler R and Co-authors (2001) The NCEP-NCAR 50-year reanalysis: monthly means CD-ROM and documentation. *Bull Am Meteorol Soc* 82: 247–267
- Malaka I, Núñez S (1980) Aspectos sinópticos de la sequía que afectó a la República Argentina en el año 1962. *Geoacta* 10: 1–21
- Metz W (1987) Transient eddy forcing of low-frequency atmospheric variability. *J Atmos Sci* 44: 3–22
- Michelangeli PA, Vautard R, Legras B (1995) Weather regimes: recurrence and quasi stationarity. *J Atmos Sci* 52: 1237–1256
- Mo K, Higgins RW (1998) The Pacific-South American modes and tropical convection during the Southern Hemisphere winter. *Mon Weather Rev* 126: 1581–1596
- Mo K, White GH (1985) Teleconnections in the Southern Hemisphere. *Mon Weather Rev* 113: 22–37
- Plaut G, Simonnet E (2001) Large-scale circulation classification, weather regimes, and local climate over France, the Alps and Western Europe. *Clim Res* 17: 303–324
- Renwick JA, Revell MJ (1999) Blocking over the South Pacific and Rossby wave propagation. *Mon Weather Rev* 127: 2233–2247
- Robertson A, Ghil M (1999) Large-scale weather regimes and local climate over western United States. *J Clim* 12: 1796–1813
- Rusticucci M, Barrucand M (2002) Climatología de temperaturas extremas en la Argentina. Parte 1: consistencia de datos. Relación entre la temperatura media estacional y la ocurrencia de días extremos. *Meteorológica*, (in press)
- Rutllant J, Fuenzalida H (1991) Synoptic aspects of the central Chile rainfall variability associated with the Southern Oscillation. *Int J Climatol* 11: 63–76
- Simmonds I, Keay K (2000) Mean Southern Hemisphere extratropical cyclone behavior in the 40-year NCEP-NCAR Reanalysis. *J Clim* 13: 873–885
- Solman S, Menéndez C (2002) ENSO – related variability of the Southern Hemisphere winter storm track over the eastern Pacific – Atlantic sector. *J Atmos Sci* 59: 2128–2140
- Thompson DWJ, Solomon S (2002) Interpretation of recent Southern Hemisphere climate change. *Science* 296: 895–899
- Trenberth K, Mo K (1985) Blocking in the Southern Hemisphere. *Mon Weather Rev* 113: 3–21
- Vautard R (1990) Multiple weather regimes over the North Atlantic: analysis of precursors and successors. *Mon Weather Rev* 118: 2056–2081